(Received 7 June 2024, Accepted 12 July 2024, Scheduled 5 August 2024)

Development and Measurement of a 3D Printable Radar Absorber

Tobias Plüss[1,*], Axel Murk[1], Diana Vorst[2], Denis Nötel[2], Martin Schürch[3], and Peter Wellig[3]

[1] *Institute of Applied Physics, University of Bern, Bern, Switzerland*
[2] *Fraunhofer-Institut für Hochfrequenzphysik und Radartechnik FHR, Wachtberg, Germany*
[3] *Armasuisse Wissenschaft und Technologie, Thun, Switzerland*

ABSTRACT: In this paper, we present our measurements about 3D printable microwave absorber materials. First, we determined the electromagnetic parameters of the material using different measurement techniques, whose some examples we present. Knowing the material parameters, a geometry for a 3D printable absorber was selected, and simulations were performed to optimise the geometry from X-band (8.2 GHz to 12.4 GHz) to Ka-band (26.5 GHz to 40 GHz). Pieces of absorbers were 3D printed using the optimised dimensions and were mounted to a metallic corner reflector as test subject. The corner reflector camouflaged in this way was then measured in an anechoic chamber, and measurements with and without the 3D printed absorbers are compared. We found good agreement between the measurements and simulations and found the structure and the material we used as usable candidates for the reduction of the radar cross section of an object.

1. INTRODUCTION

Microwave absorbers are used for many different applications. In this paper, we focus on an application to reduce the radar cross section (RCS) of an object by placing an absorbing structure on the object. This can be used, for example, on a vehicle, to reduce its RCS by placing absorber structures at strategic locations. Typical designs of absorber structures are pyramids, graded interfaces, or resonant materials such as the Salisbury screen [1].

On the other hand, 3D printing technology offers various advantages, such as rapid prototyping and cheap manufacturing, even of very complicated structures. Therefore, it is desirable to have the ability of producing a microwave absorber that can be 3D printed. This will allow an absorber structure to be optimised, not only in terms of its electromagnetic properties but also in its shape and dimensions such that it can be applied for a specific use case [2–6].

In this work, we looked at commercially available materials that are possible candidates for 3D printable absorber geometries. We measured the electromagnetic material parameters and then used this to optimise a 3D structure with the aid of finite element (FEM) simulations in Ansys HFSS (high frequency structure simulator) for good absorption in X-band and Ka-band. After the geometric parameters of the structure were optimised for good absorption, we printed the structure and mounted it on top of a planar metallic reflector to test its absorption. Then, we proceeded and mounted the structure on the inside of a corner reflector to demonstrate the usage in a more typical application. We measured the RCS of the corner reflector in an anechoic chamber for various incidence angles and polarisations, with and without the absorber structure mounted, and compared the results with the simulations. We could observe that the 3D printed structure provided a significant reduction of the RCS of the corner reflector and therefore could be suitable for RCS reduction of vehicles or objects. Further, our structure has several advantages, compared to other microwave absorbers:

- the structure can be vented since it has large holes. Therefore, it is suitable for being placed on devices that produce heat and therefore need to be cooled by airflow.
- the structure is lightweight, due to the aforementioned holes.
- as 3D printing is used, it is cheap to print the absorber structure, and the materials and/or the geometry can be changed easily, as dictated by the application.
- a frequency range from X-band to Ka-band was tested, with good results. Therefore, the structure exhibits good broad-band absorption properties.

2. MEASUREMENTS AND SIMULATIONS

2.1. Material Parameter Measurement

We performed a detailed study of various commercially available 3D printable materials and measured their electromagnetic material parameters using different methods and tried to investigate in their composition using scanning electron microscope (SEM) images. For example, the SEM images allow to qualitatively compare structural details of the materials, such as distribution of grains, their shape, and so on. The full paper where

* Corresponding author: Tobias Plüss (tobias.pluess@unibe.ch).

we presented all materials, as well as the measurement methods and the results is available in [7], and therefore, we give here only a brief summary.

To measure the material parameters, small coaxial and rectangular test specimens were 3D printed and then inserted into either a coaxial transmission line or a piece of WR90 waveguide.

For example, the coaxial test setup uses a piece of coax transmission line where the material under test (MUT) is placed inside. Fig. 1 shows a photograph of the transmission line with a material sample.

FIGURE 1. Coaxial sample holder and material sample.

The assembled transmission line is then connected to a Rohde & Schwarz ZVA40 network analyzer as shown in Fig. 2 for the measurement of the transmission (S_{21}, S_{12}) and reflection (S_{11}, S_{22}) S-parameters.

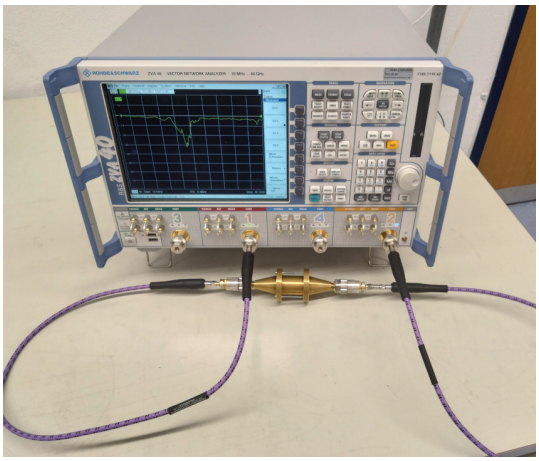

FIGURE 2. Coaxial sample holder with material sample inside, connected to the network analyzer.

We employed the "Baker-Jarvis reference plane invariant method" [8] to extract the permittivity of the material under test. Refer to [7] for further details about these measurements and how the measured data is processed.

From all materials we tested polylactic acid filled with carbon black, iron, or stainless steel and found that the "Protopasta CDP12805" (carbon filled) was the most suitable due to high dielectric losses and good quality of the printout. Also, the magnetic losses that the other materials exhibit did not provide a significant improvement of the overall electromagnetic losses. The permittivity of this material is shown in Fig. 3. It is a non-magnetic material; therefore, the permeability is 1. For our simulations, where we want to optimise the geometry for X-band, we observe that the permittivity is almost constant, and therefore, we used the values $\epsilon_r' = 10.5$ and $\epsilon_r'' = -7$.

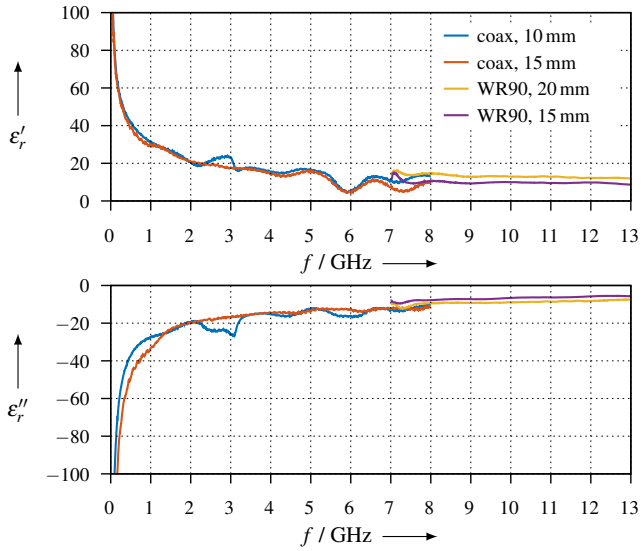

FIGURE 3. Permittivity of the Protopasta CDP12805 material, two different sample lengths each measured with the waveguide and with the coaxial setup.

2.2. Simulations

We simulated, printed, and tested a couple of different geometries similar to [3–5]. For our purposes, we found that the honeycomb structure was the most suitable for our use case. To optimise the structure for optimal return loss, we conducted FEM simulations on a unit cell only. The software package "High Frequency Structure Simulator" (HFSS) from Ansys was used for the simulations. The unit cell of the geometry we employed is shown in Fig. 4. We simulate the return loss of the structure when a electromagnetic wave is incident from the top. Further, note that the bottom wall of the unit cell is specified as perfect electric conductor (PEC), because we want to place our absorber structure later on top of a metal sheet.

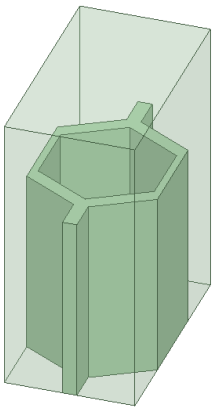

FIGURE 4. Unit cell as simulated in HFSS.

With the aid of the simulation, we tried to optimise the dimensions of the structure (inner side length of the honeycomb cell, wall thickness, height) such that we achieve a return loss of around −10 dB from X through K band. With an inner side length of 5 mm, a wall thickness of 3 mm, and a height of 10 mm, the simulation predicts a return loss as shown in Fig. 5.

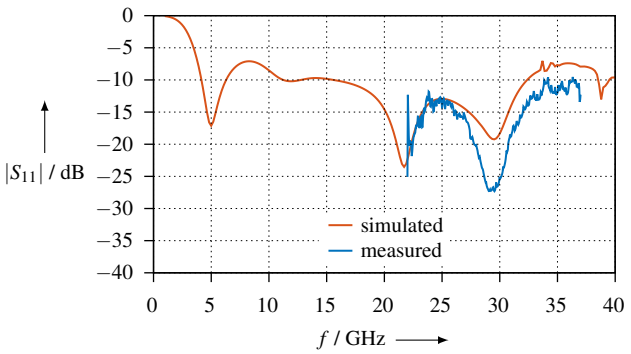

FIGURE 5. Comparison of the simulated and the measured return loss in Ka band.

We verified our simulation by printing a piece of the structure and measuring in front of a corrugated horn antenna. This provides a good approximation of a free-space measurement at normal incidence. A photograph of our test setup is shown in Fig. 6.

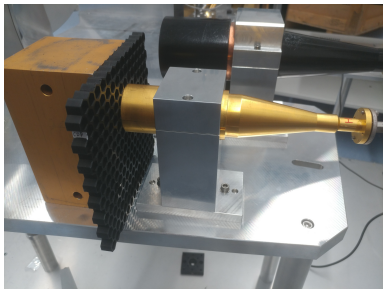

FIGURE 6. Measurement of a piece of 3D printed honeycomb absorber in front of a corrugated horn antenna.

Figure 5 shows a comparison of the simulated and measured return losses. As at the time the measurement was taken no corrugated antenna for X-band was available but only for Ka-band, we have shown only the measurement in Ka band. We observe good agreement between the simulation and measurement.

2.3. Simulation and Measurement of a Corner Reflector

To demonstrate that the honeycomb structure is suitable as a microwave absorber and effectively reduces the RCS of an object, we chose a corner reflector as test subject because the corner reflector has a comparably high RCS, and there are closed-form models that describe the RCS of a corner reflector, i.e., we can easily validate our measurement. Again we start with a simulation. Fig. 7 shows the geometry of the corner reflector, where the honeycomb absorbers are placed on the inside. The side length of the corner reflector is 200 mm.

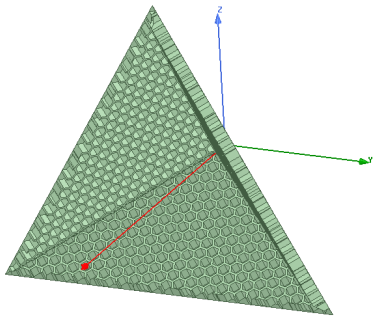

FIGURE 7. Corner reflector, with honeycomb absorber structure placed inside.

Further, we also performed a measurement of an actual corner reflector with the same 200 mm side length in the anechoic chamber at Fraunhofer FHR. The RCS was measured using a quasi-monostatic test setup, i.e., two separate, but closely spaced transmitting and receiving antennas were used. A picture of the anechoic chamber and antennas is shown in Fig. 8.

A picture of the antennas used is shown in Fig. 9. The used rectangular horn antennas are mounted next to each other on an antenna holder. The antennas look into the anechoic chamber through a window and are, on the outside of the anechoic chamber, connected to a network analyzer using waveguide to coax adaptors.

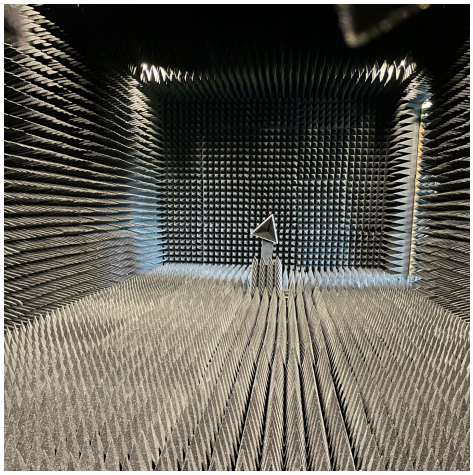

FIGURE 8. Anechoic chamber at Fraunhofer FHR. Mounted on the test stand is the metallic corner reflector with honeycomb absorbers put inside.

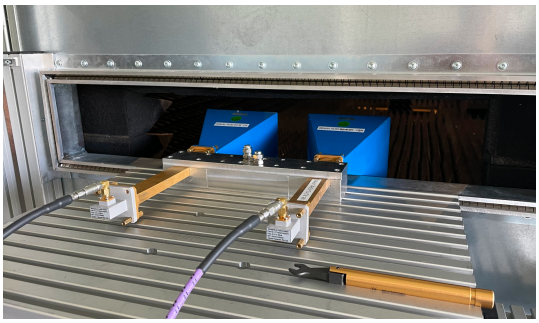

FIGURE 9. Horn antennas.

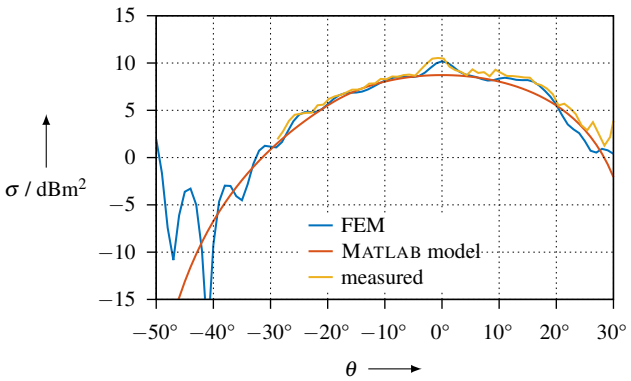

FIGURE 10. Comparison of the measurement and the simulation for X-band, without absorbers in place, vertical polarisation, elevation angular sweep.

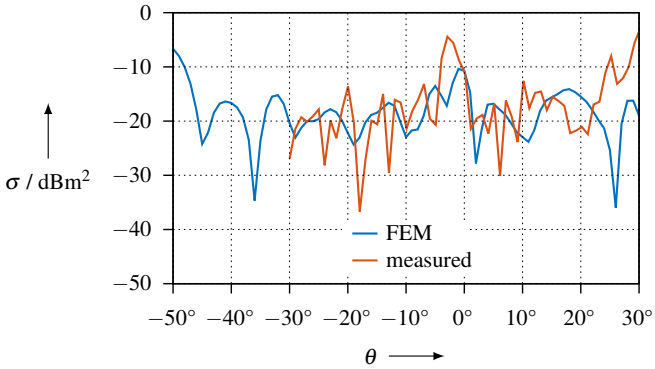

FIGURE 11. Comparison of the measurement and the simulation, with absorbers in place, elevation angular sweep.

With the network analyzer, the transmission S_{21} between the two antennas is measured as the corner reflector is rotated. A calibration procedure is employed to determine the RCS of the device under test (DUT) from the measured S_{21}. The calibration procedure is required because there are numerous error sources. The following steps explain the calibration procedure.

1. one measurement is taken when the anechoic chamber is completely empty. This measurement takes into account the direct crosstalk between the two antennas and reflections inside the chamber, and is denoted as $S_{21,\text{empty}}$.

2. one further measurement is taken when there is a square aluminium plate with known side length as the DUT. Since the RCS of the square plate can be computed easily, the offset for converting S_{21} to RCS can be determined. This measurement is denoted as $S_{21,\text{cal}}$ and is needed to take into account the gain of the horn antennas, the path loss from the antennas to the DUT and back, and cable losses. The RCS of the known square plate is denoted as σ_{cal}.

Then, to obtain the measured the RCS of the DUT from the measured S_{21}, the following correction is applied

$$\sigma_{\text{DUT,dBm}^2} = 20\log\left(S_{21} - S_{21,\text{empty}}\right) - S_{21,\text{cal,dB}} + \sigma_{\text{cal,dBm}^2} \quad (1)$$

which directly converts the measured S_{21} to σ of the DUT.

3. RESULTS

In this section, we compare the simulations and measurements of the corner reflector's RCS. To validate our measurement, for the "blank" corner reflector, i.e., without honeycomb absorber in place, we also compare them with a closed-form model [9] that we implemented in MATLAB. We present in this section a small excerpt of the measurement data we obtained that is representative. Measurements performed for other polarisations and in different frequency bands look similar to the ones presented here.

Figure 10 shows the comparison of the measurement at 10 GHz, the MATLAB model, and the RCS measurement when the honeycomb absorber is not in place. This is for X-band and vertical polarisation, and the corner reflector was rotated in the elevation by $\pm 30°$. We note very good agreement among all three, measurement, FEM simulation, and MATLAB model. Also interesting to note is the little "bump" at $0°$. Since this is present in both, the FEM simulation and the measurement, we conclude that this is not a simulation artifact but instead a true property of the corner reflector. This effect is not present in the MATLAB model; this is something that one needs to be aware of in case one uses a corner reflector for calibration purposes.

Figure 11 shows the comparison of the simulation and the RCS measurement at 10 GHz after the 3D printed absorber structure has been placed inside the corner reflector. For this situation, we do not have a closed form model, but it can be clearly observed that the FEM simulation and measurement have quite good agreement. Also, a reduction of the RCS about 15 dB can be observed, thanks to the 3D printed absorber that is placed.

Similarly, Fig. 12 shows the RCS of the corner reflector when it rotated in azimuth by $\pm 30°$. As before, we observe very good agreement among the FEM simulation, MATLAB model, and measurement.

For the measurement when the absorber structure is in place, refer to Fig. 13. The agreement between the measurement and FEM simulation is still good, and we also note around 15 dB reduction of the RCS when the absorber is in place.

Figure 14 shows a frequency sweep for the blank corner reflector (i.e., no absorbers in place) where the FEM model, MATLAB model, and measurements are compared. We observe good agreement between the FEM result and MATLAB model; however, the simple MATLAB model does not exhibit the ripple. Also we have generally good agreement between the measurements and simulations; the deviation that becomes larger for the higher frequencies is most likely because the measurement setup is not truly monostatic.

In contrast to that, a significant RCS reduction can be observed in the frequency sweep that is shown in Fig. 15. Here, the absorbers are in place. For reference, we have again plotted the RCS of the uncoated corner reflector, such that one can easily compare the RCS of the uncoated vs. the coated reflector. We observe generally a good agreement between the measurements and simulations.

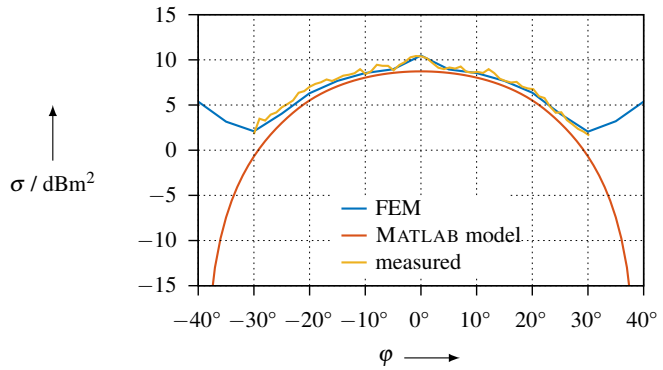

FIGURE 12. Comparison of the measurement and the simulation for X-band, without absorbers in place, vertical polarisation, azimuth angular sweep.

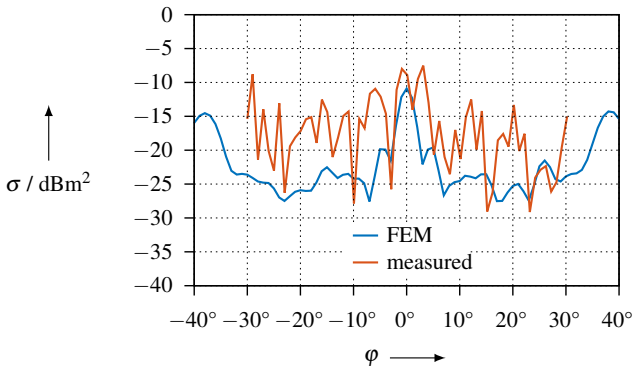

FIGURE 13. Comparison of the measurement and the simulation for X-band, with absorbers in place, vertical polarisation, azimuth angular sweep.

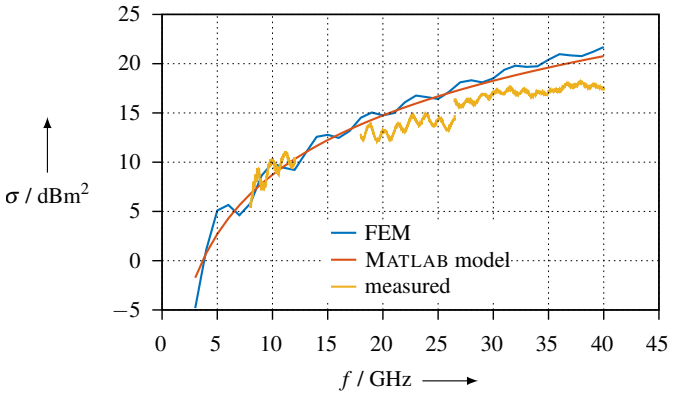

FIGURE 14. Comparison of the measurement and the simulation for a frequency sweep at normal incidence, without absorbers in place.

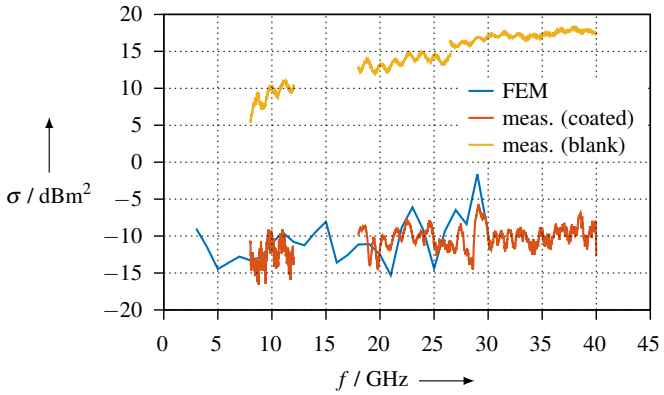

FIGURE 15. Comparison of the measurement and the simulation for a frequency sweep at normal incidence when the absorbers are in place.

4. CONCLUSIONS

We have measured the material properties of 3D printed absorber materials and selected the material that is a suitable candidate for the 3D printing of radar absorbers. We then looked at different possible geometries and selected one of them. The geometry was optimised for approximately 10 dB RCS reduction, and a test specimen of the geometry was printed. When the printed geometry was put inside a corner reflector for measurement, we observed a reduction of the RCS of the corner reflector of around 15 dB at 10 GHz. The measurements were validated by also measuring the corner reflector without the absorber in place and comparing it with an FEM simulation and a closed-form MATLAB model.

ACKNOWLEDGMENT

This work has been funded by armasuisse W+T. Also, we thank our colleagues at FHR for providing access to the FHR facilities for the measurements.

REFERENCES

[1] Saville, P., *Review of Radar Absorbing Materials*, Defence Research & Development Canada, Defence R & D Canada-atlantic, 2005.

[2] Lu, Y., B. Chi, D. Liu, S. Gao, P. Gao, Y. Huang, J. Yang, Z. Yin, and G. Deng, "Wideband metamaterial absorbers based on conductive plastic with additive manufacturing technology," *ACS Omega*, Vol. 3, No. 9, 11 144–11 150, 2018.

[3] Ren, J. and J. Y. Yin, "3D-printed low-cost dielectric-resonator-based ultra-broadband microwave absorber using carbon-loaded acrylonitrile butadiene styrene polymer," *Materials*, Vol. 11, No. 7, 1249, Jul. 2018.

[4] Jiang, W., L. Yan, H. Ma, Y. Fan, J. Wang, M. Feng, and S. Qu, "Electromagnetic wave absorption and compressive behavior of a three-dimensional metamaterial absorber based on 3D printed honeycomb," *Scientific Reports*, Vol. 8, No. 1, 4817, Mar. 2018.

[5] Petroff, M., J. Appel, K. Rostem, C. L. Bennett, J. Eimer, T. Marriage, J. Ramirez, and E. J. Wollack, "A 3D-printed broadband millimeter wave absorber," *Review of Scientific Instruments*, Vol. 90, No. 2, 024701, 2019.

[6] Laur, V., A. Maalouf, A. Chevalier, and F. Comblet, "Three-dimensional printing of honeycomb microwave absorbers: Feasibility and innovative multiscale topologies," *IEEE Transactions on Electromagnetic Compatibility*, Vol. 63, No. 2, 390–397, 2021.

[7] Plüss, T., F. Zimmer, T. Hehn, and A. Murk, "Characterisation and comparison of material parameters of 3D-printable absorbing materials," *Materials*, Vol. 15, No. 4, 1503, 2022.

[8] Baker-Jarvis, J., E. J. Vanzura, and W. A. Kissick, "Improved technique for determining complex permittivity with the transmission/reflection method," *IEEE Transactions on Microwave Theory and Techniques*, Vol. 38, No. 8, 1096–1103, 1990.

[9] Doerry, A. W., "Reflectors for SAR performance testing," Tech. Rep., 2014.